

Document downloaded from:

<http://hdl.handle.net/10251/116798>

This paper must be cited as:

Luna Molina, R.; Domingo Beltran, M.; Millán Verdú, C.; Santonja Moltó, MDC.; Satorre, MÀ. (2018). Study of the frequency factor in the thermal desorption of astrophysical ice analogs: CH₄, C₂H₄, C₂H₆, CH₃OH, CO, CO₂, H₂O and N₂. *Vacuum*. 152:278-284.
doi:10.1016/j.vacuum.2018.03.022



The final publication is available at

<http://doi.org/10.1016/j.vacuum.2018.03.022>

Copyright Elsevier

Additional Information

Study of the frequency factor in the thermal desorption of astrophysical ice analogs: CH₄, C₂H₄, C₂H₆, CH₃OH, CO, CO₂, H₂O and N₂.

R. Luna^a, M. Domingo^a, C. Millán^a, C. Santonja^a, M. Á. Satorre^a

^a*Centro de Tecnologías Físicas. Universitat Politècnica de València, 46022 València, Spain
e-mail: ralunam@fis.upv.es*

Abstract

In this work the frequency factor and the influence of the temperature on this parameter, for zeroth order desorption processes, has been experimentally determined for eight molecules of astrophysical interest. In the literature, this parameter has been estimated indirectly, obtaining values that differ by as much as three orders of magnitude from different authors. As a consequence, there are very different desorption rates reported for the same molecule and additionally its temperature dependence has been systematically neglected.

The frequency factor is widely used to model the dynamics of these species under low temperature conditions present in some astrophysical environments. The method reported in this work is based on the analysis of the signal of a quartz crystal microbalance acting as a sample-holder, which is able to directly detect molecules desorbing from it.

Two different types of desorption experiments were necessary for this study. In a first set of experiments, carried out at a constant rate of warming up, the desorption energy is obtained. The second set of experiments were performed at several constant temperatures to calculate the frequency factor and its relationship with temperature. The reasons for some anomalous behaviour have been analyzed. The dependence of the frequency factor on temperature should be taken into account when the Polanyi-Wigner equation is used for desorption processes. Every molecule has to be independently studied as no global tendency is found for the variation of the frequency factor with temperature.

Key words: ice films, sublimation processes, experimental laboratory

1. Introduction

Some astrophysical scenarios are cold enough for the molecules to be in solid state, for instance: molecular clouds in the interstellar medium, protostellar clouds, circumstellar matter of post AGB stars, satellites, TNOs and comets. Ices present in these environments are exposed to the possibility of sublimation if any input of energy (photons, ions, grain shocks, etc) occurs. In particular, the thermal desorption process is widely modelled by the Polanyi-Wigner equation [1]:

$$-\frac{dN}{dt} = A_i \cdot N^i \cdot \exp\left(-\frac{E_{des}}{R \cdot T}\right) \quad (1)$$

where N (in *molecule cm⁻²*) is the amount of molecules present onto the surface, i is the order of the process, A_i is the frequency factor, the product “ $A_i \cdot N^i$ ” is called pre-exponential factor, E_{des} is the desorption energy, T is the absolute temperature and R is the constant for ideal gases.

This equation can be applied to desorption processes to determine, for instance: surface coverage, residence time, desorption energy or sublimation rate of molecules from the ice bulk. Additionally, this equation can be used to determine the order of the process for a molecule, which is usually an integer $i = 0, 1, 2, \dots$, although some authors have even obtained a non-integer number [2].

In the literature, different values for A_i have been reported [3–6]. They were estimated from an experiment designed to obtain E_{des} fitting the experimental desorption curve. Despite the fact that temperature increases during these desorption experiments, a constant value has been assumed for the frequency factor. However, A_i depends on the temperature, as has been theoretically explored by different authors [7,8].

An experimental study, for a single molecule, was carried out in a previous work for the case of C_2H_6 [9]. This work evidenced the dependence of the frequency factor with the temperature, showing a clear increase of the former as the latter increases. The present work is intended to extend this study to a set of eight molecules of astrophysical interest to test whether this is a general trend.

The molecules selected for this study are: CH_4 , C_2H_4 , C_2H_6 , CH_3OH , CO , CO_2 , H_2O and N_2 . The case of CH_3OH has been addressed in a previous work [10] and is used here for comparison purposes. These molecules cover a wide range of desorption energies ($4.3 - 47 \text{ kJ mol}^{-1}$).

The experimental conditions used in the present work lead to a zeroth-order desorption process characterized by multilayer deposits. Therefore, this work is only focused on studying the frequency factor dependence on temperature for zeroth-order desorption processes.

The layout of this article is as follows. Section 2 contains a description of the experimental setup, section 3 presents the experimental procedure and results are subsequently discussed in section 4. Finally, the conclusions are presented in section 5.

2. Experimental Setup

The experiments performed were carried out in a system working under high vacuum (HV) conditions. The main components were a quartz crystal microbalance (QCMB), a double laser system (DLS) and a temperature controller (Fig. 1).

The base pressure during the experiment ($3 \cdot 10^{-8}$ mbar) was obtained by assembling a pair of turbomolecular pumps backed by their corresponding rotary pumps and the help of a closed-cycle He cryostat acting as a cryopump. To obtain a constant flow of molecules entering the chamber, two parameters were regulated: the pressure in the pre-chamber (measured with a capacitive sensor) and the aperture of a needle valve at the entrance.

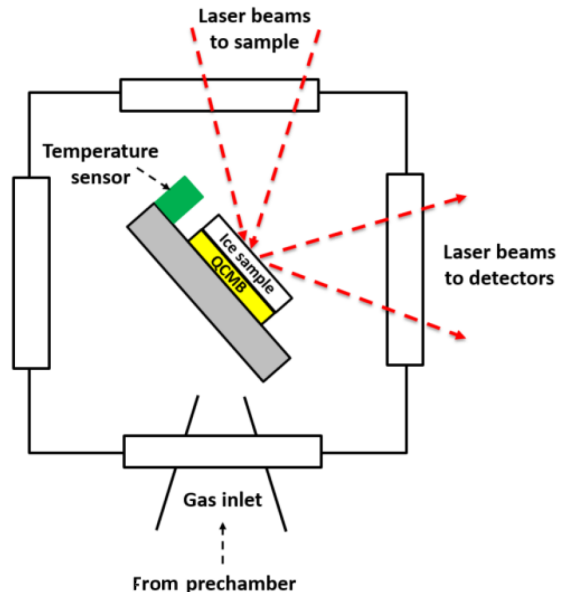


Fig. 1. Main components of the experimental setup. Disposition of the laser beams and location of the QCMB, the sample, and one of the temperature sensors.

The edge of the cryostat was in thermal contact with the QCMB (Q-Sense gold coated quartz, 5 MHz). The temperature of the sample (deposited onto the QCMB) was governed by an ITC 503S intelligent temperature controller (Oxford Instruments), using two silicon diode sensors (Scientific Instruments), with one located just beside the quartz crystal and the other one placed beside the heating resistor. The arrangement formed by the ITC and a resistor allowed the temperature to be varied between 13.0 and 300.0 ± 0.1 K, by means of a resistor. To measure the film thickness during the growth, interferometric patterns were obtained by means of a double laser He-Ne (632.8 nm) interferometric system (DLI). A more detailed description of the experimental setup can be consulted at [11].

3. Experimental Procedure and Results

The procedure used in this work is already reported in [9], here is only described in short. Two different types of experiments were carried out.

3.1. Desorption at a constant heating rate

Desorption energy is a parameter that represents an input necessary to calculate the frequency factor of a molecule. Therefore, as a first step, this quan-

tity has to be determined. With this purpose, desorption experiments at a constant rate of warming up were performed. For each molecule, the experiment was repeated at least 5 times in order to estimate the uncertainty of the values obtained. The raw signal recorded during deposition and thermal desorption for carbon monoxide is shown in Fig. 2. The QCM frequency signal (solid line) and temperature (dashed line) versus time are plotted in this figure. During the time period between 4800 and 6100 s, the ice growth takes place. The starting point of the deposition is at approximately 4800 s, when the frequency signal starts to decrease with a constant slope due to a constant rate of mass deposition onto the QCM over the sample holder. The Sauerbrey equation [12] $\Delta F = -S \cdot \Delta m$, represents the relationship between the QCM frequency variation (ΔF) and the variation of the deposited mass (Δm) through the constant S of our system. The thickness of the film was controlled by means of the interference pattern obtained with the DLI. Fig. 3 shows the interference fringes obtained during the deposit of nitrogen. When a thickness of approximately $2.0 \mu\text{m}$ was achieved, the deposition was stopped. The other relevant period in the experiment corresponds to the desorption process which starts at approximately 6500 s in Fig. 2 (when the dashed line starts to rise), with a heating rate of 1 K min^{-1} as is widely used by other authors for similar studies. From the QCM signal recorded in the interval from 6500 to 7700 s (solid line), it is possible to derive the desorption energy. The raw frequency signal was corrected with the removal of two effects which are inherent to these experiments: the influence of the temperature on the QCM frequency signal and the variation in frequency due to the presence of contaminants (mainly water). The procedure is explained in detail in [13].

Once the signal was corrected, the desorption energy was calculated from the Polanyi-Wigner equation, adapted to a zeroth order desorption process:

$$r_{des} = A_0 \cdot \exp\left(-\frac{E_{des}}{R \cdot T}\right) \quad (2)$$

where r_{des} is the desorption rate ($-\text{dN}/\text{dt}$) of molecules from the QCM. The value of r_{des} was obtained from the derivative of the frequency versus time for the signal presented in Fig. 2 (solid line for time higher than 6500 s). The result obtained is shown in Fig. 4 for the case of carbon dioxide, where r_{des} is plotted against temperature. From the profile of the curve it is possible to confirm the

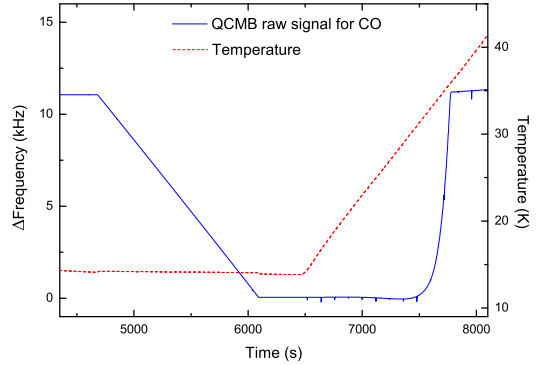


Fig. 2. The raw QCM signal during deposition at constant temperature (time lower than 6100 s) and desorption at a constant heating rate of 1 K min^{-1} (time higher than 6500 s) for CO.

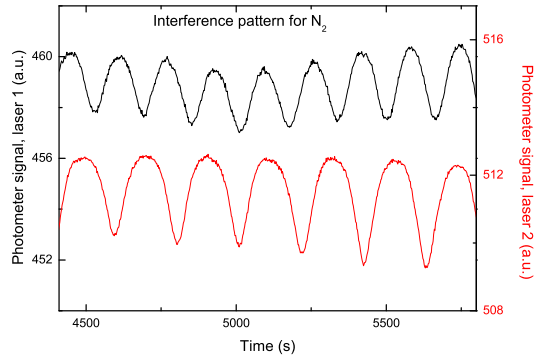


Fig. 3. Interference patterns for N_2 obtained with a double laser system during constant deposition rate and temperature.

assumption of a zeroth-order desorption process, typical of a multilayer desorption. The same profile has been obtained for all the molecules under study.

Taking the natural logarithm in Eq. (2), a linear expression is obtained:

$$\ln(r_{des}) = \ln(A_0) - \frac{E_{des}}{R} \cdot \frac{1}{T} \quad (3)$$

Therefore, a plot of $\ln(r_{des})$ versus $1/T$ leads to a straight line whose slope is $-E_{des}/R$ (see Fig. 5 for methane). From the slope, the E_{des} is derived. In Table 1, we present the desorption energy values obtained for the eight molecules under study and the temperature at which the maximum desorption rate was obtained (called hereafter desorption peak or T_{peak}).

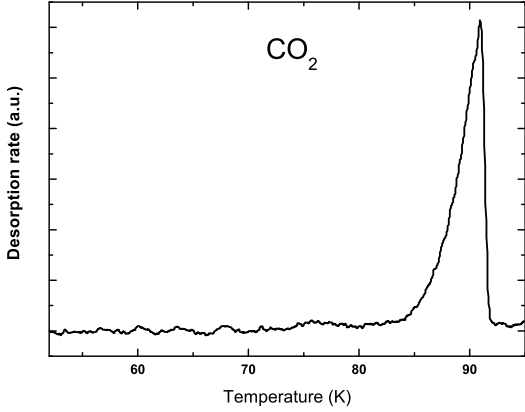


Fig. 4. Desorption rate for CO₂ during a desorption experiment performed at a constant heating rate.

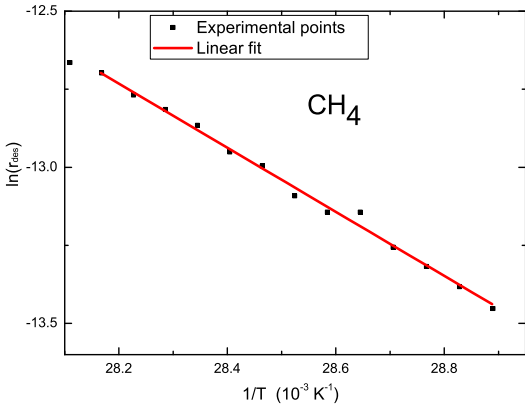


Fig. 5. Plot of $\ln(r_{des})$ versus $1/T$ (solid squares) and the linear fit (solid line) for CH₄.

3.2. Desorption at different constant temperatures

To study how temperature influences A_0 , an additional set of experiments at different selected constant temperatures was performed. These temperatures were selected to be close to the temperature of the desorption peak (column 3 in Table 1) obtained under the experimental conditions used in this work. Fig. 6 represents the QCMB signal obtained for the desorption of ethylene at three different constant temperatures (63, 65 and 67 K).

These temperatures are within the range of temperatures selected for this molecule. The interval of temperatures used for each molecule depends on our experimental conditions, so that it was possible to obtain a reasonable desorption rate which can be measured in the laboratory. In Fig. 6 it is possible to

Table 1
Calculated E_{des} and temperature for the desorption peak (T_{peak}) for eight different molecules.

Molecule	E_{des} (kJmol ⁻¹)	T_{peak} (±1 K)
Nitrogen	4.3±0.2	27
Carbon monoxide	6.3±0.3	32
Methane	8.5±0.4	40
Ethylene	19.3±1.0	70
Ethane	15.3±0.8	74
Carbon dioxide	29.3±1.5	95
Methanol	46.2±2.3	163
Water	47.0±2.4	186

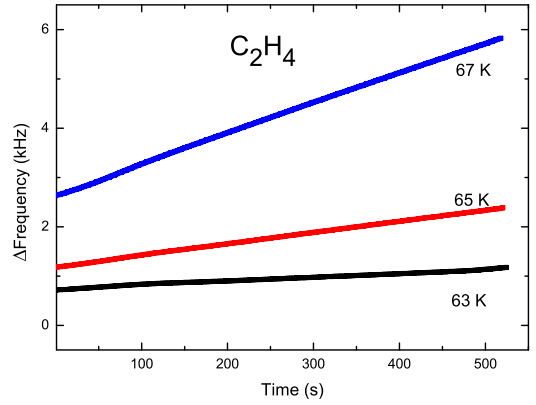


Fig. 6. QCMB experimental points during three different desorption experiments for C₂H₄ at three different constant temperatures.

observe how desorption rate increases (higher slope) as the temperature selected to perform the desorption increases.

From the analysis of the signal obtained for each temperature, A_0 is derived from the corresponding experiment, as follows:

$$A_0 = \frac{r_{des}}{\exp\left(\frac{-E_{des}}{R \cdot T}\right)} \quad (4)$$

where r_{des} was experimentally calculated as

$$r_{des} = \frac{-\Delta N}{\Delta t} = \frac{-\Delta F}{\Delta t} \cdot \frac{\Delta m}{\Delta F} \cdot \frac{1}{M_r} \cdot N_A \quad (5)$$

where Δt is the experimental interval of time, $\frac{\Delta m}{\Delta F}$ is S⁻¹ (S is the Sauerbrey constant mentioned in Section 3.1), M_r is the molar mass and N_A is the Avogadro number. Finally

$$r_{des} = \frac{-(F_2 - F_1)}{t_2 - t_1} \cdot S^{-1} \cdot \frac{1}{M_r} \cdot N_A \quad (6)$$

where F_1 , t_1 , and F_2 , t_2 are the corresponding values for the frequencies and times at the starting and ending points respectively for the straight lines obtained from the QCMB signal during the desorption at a constant temperature (see Fig. 6 for the cases of 63, 65 and 67 K). Fig. 7 shows all the experimental values obtained for each molecule. Each point represents the value of the frequency factor calculated from every single desorption experiment at a selected constant temperature.

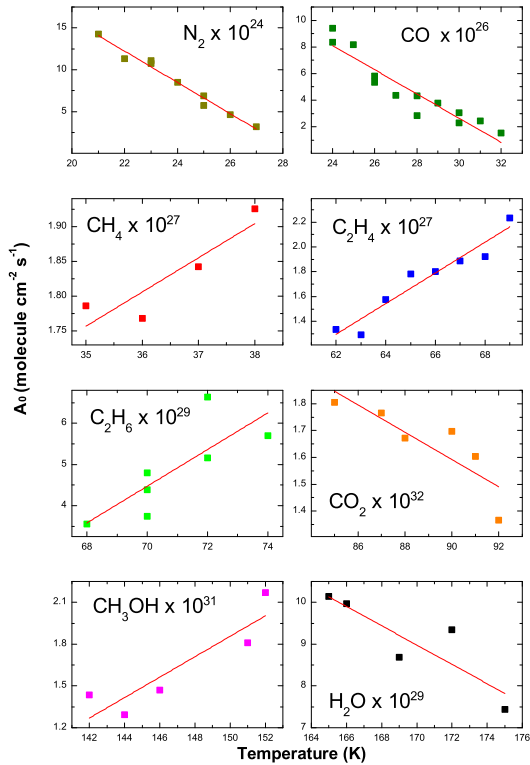


Fig. 7. Detail of the frequency factor versus temperature for the eight molecules under study. Solid lines represent the linear fits for the frequency factor versus temperature.

4. Discussion

In a previous work [9], the dependence of frequency factor with temperature was studied for the first time. It was found that, for C_2H_6 , the frequency factor increases as temperature increases. Therefore, it seems necessary to check whether this is a general behaviour. The results obtained for the case of

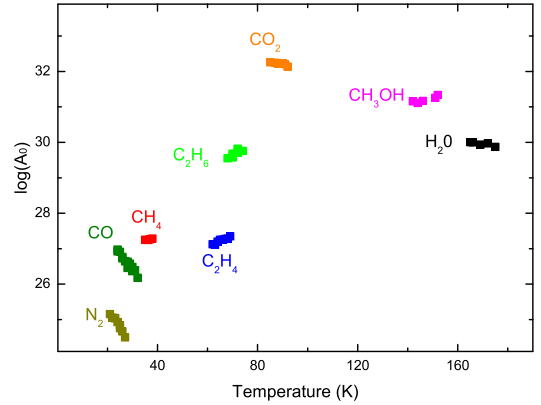


Fig. 8. Comparison of the frequency factor versus temperature for eight molecules of astrophysical interest.

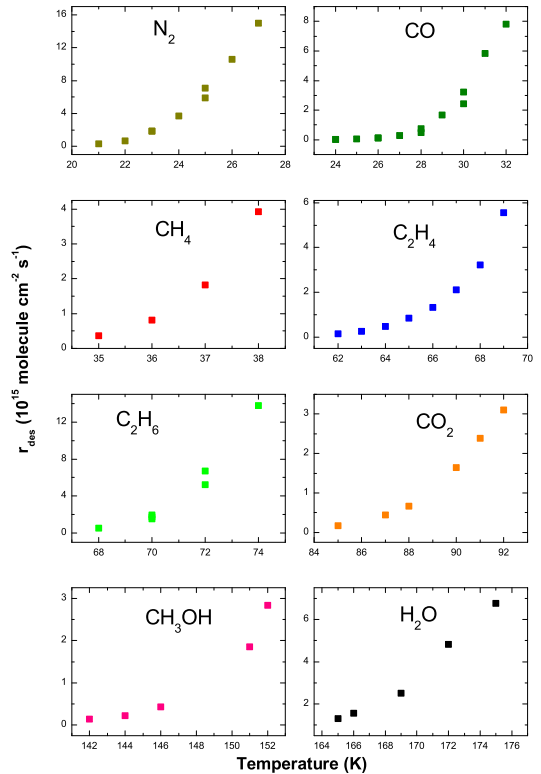


Fig. 9. Experimental desorption rate versus temperature for the molecules under study.

C_2H_6 are studied together with a selected group of molecules.

In Fig. 8, the frequency factor values for all the species studied have been plotted in the same graph. As a first result, it can be observed that, in general terms, the frequency factor is higher for molecules

with higher desorption energy. The values obtained are within the range 10^{24} to 10^{33} ($\text{molecule cm}^{-2} \text{ s}^{-1}$). Some deviations to this trend can be observed. At first sight, it appears that CO_2 presents values for frequency factor higher than those expected from its E_{des} . However, it seems more plausible assuming that the more refractory water and methanol ices have lower A_0 values than expected. This is likely due to their hydrogen bonds, which implies a higher molecular interaction that could slow down the desorption of these molecules.

Taking a deeper look at all the molecules in the panels of Fig. 7, it is possible to observe two different types of behaviour: there are four molecules (methane, ethylene, ethane, and methanol) whose frequency factor increases as temperature increases, and there are four molecules whose frequency factor decreases as temperature increases (nitrogen, carbon monoxide, carbon dioxide, and water). Therefore, there are at least four molecules in this group behaving in an opposite way from the theoretical increase expected when temperature increases as stated in the introduction.

From Eq. (4), A_0 is obtained as the ratio between the experimental desorption and an exponential expression that increases with temperature. Then, the tendency of this quotient (increasing or decreasing) depends on how these factors relatively vary one from the other. Therefore, it is worth exploring apart the behaviour of the experimental desorption rate with temperature. Fig. 9 represents the experimental desorption rate for the molecules studied, clearly showing that desorption rate increases as temperature increases. Therefore, the increasing desorption rate with temperature is lower than the exponential influence of the temperature for the cases of nitrogen, carbon monoxide, carbon dioxide, and water.

The observed behavior of the frequency factor might be related to molecular interactions and/or changes in the spatial configuration of the solids. Molecular interactions can be discarded because these ices, with an unexpected behaviour, are non-polar, polar, and hydrogen-bond. If the geometric configuration is taken into account, it is reasonable to conclude that all these molecules are planar (or linear). Nevertheless, C_2H_4 is also planar and does not belong to the group with an anomalous behavior. Therefore, from our experiments, it is not possible to associate this effect to specific geometric configuration and it is not possible to predict the effect of temperature on A_0 for a specific species. Instead, it is necessary to study every molecular ice

Table 2
Expression obtained for A_0 and its temperature validity range for the eight molecules selected in this work.

Molecule	A_0 ($\text{molecule cm}^{-2} \text{ s}^{-1}$)	Validity range (K)
N_2	$-1.87\text{E}24 \cdot T + 5.33\text{E}25$	21-27
CO	$-9.11\text{E}25 \cdot T + 3.00\text{E}27$	24-32
CH_4	$1.23\text{E}25 \cdot T + 1.36\text{E}27$	36-39
C_2H_4	$1.24\text{E}26 \cdot T - 6.38\text{E}27$	62-69
C_2H_6	$4.45\text{E}28 \cdot T - 2.67\text{E}30$	68-74
CO_2	$-5.08\text{E}30 \cdot T + 6.17\text{E}32$	85-92
CH_3OH	$7.33\text{E}29 \cdot T - 9.14\text{E}31$	142-152
H_2O	$-2.31\text{E}28 \cdot T + 4.83\text{E}30$	165-175

individually to estimate the values of this parameter.

From the plot obtained in Fig. 7, it is assumed that A_0 varies linearly with temperature within the interval studied. The expression obtained with the linear fit is reported in Table 2 (column 2). In this table, column 3 represents the temperature validity range of that expression.

Using the expressions obtained in Table 2 for the frequency factor, a relative variation (between the highest and the lowest value) from 0.09 to 5.2 was found, depending on the molecule, within a variation of 10 K at most. This fact reinforces the idea that the variation of the frequency factor with temperature has to be taken into account when calculations related to desorption processes are performed.

5. Conclusions

Among other applications, the Polanyi-Wigner equation is widely used to calculate the desorption rate for ices under astrophysical conditions. The frequency factor is a parameter present in this equation. In the literature, this parameter has been estimated, providing a large interval of values for the same molecule. Additionally, a negligible variation with temperature for the frequency factor has been assumed but this assumption has not been checked experimentally.

In this paper the experimental results of the frequency factor for a zeroth-order desorption process (typical of a multilayer desorption) for eight molecules which cover a wide range of desorption energies are presented. Additionally, the authors studied how temperature influences this parameter, which is necessary to use the Polanyi-Wigner equation. To this aim, an analysis of the QCM signal

was used. This instrument is used as a sample-holder and it is used to detect and measure directly the molecules that abandon its surface. The study presented in this work has been based on two different types of experiments, based on desorption experiments either at constant heating rate or at constant temperature.

As a first result, it was found that, in general, frequency factor can be expected to be higher for molecules with higher E_{des} . Nevertheless, the presence of intermolecular forces could decrease the value of this parameter.

Additionally, studying the behaviour with temperature for every single molecule, two different trends are observed: increasing or decreasing with temperature; but no specific reasons have been found to this in each group. All the experimental points, for each molecule, were fitted to a linear trend. Relative variations, for a particular molecule, up to 5.2 for the frequency factor were obtained, even for the small range of temperature that can be studied in the laboratory.

This work demonstrates that temperature clearly influences the frequency factor. The relationship between the frequency factor and temperature for every molecule has to be studied separately as no global tendency was found.

The results presented are relevant to carry out a more accurate use of the Polanyi-Wigner equation when a desorption process close to its desorption temperature is studied.

Acknowledgments

This work was supported by the Plan Nacional FIS2013-48087-C2-2-P and FIS2016-77726-C3-3-P of the Ministerio de Economía y Competitividad (co-financed by FEDER funds).

References

- [1] M. Polanyi, E. Wigner, Bildung und Zerfall von Molekülen, *Z. Physik* 33 (1925) 429-434.
- [2] W.A. Brown, A.S. Bolina, Fundamental data on the desorption of pure interstellar ices, *Mon. Not. R. Astron. Soc.* 374 (2007) 1006-1014.
- [3] M.P. Collings, J.W. Dever, H.J. Fraser, M.R.S. McCoustra, Laboratory studies of the interaction of carbon monoxide with water ice, *Astrophys. Space Sci.* 285 (2003) 633-659.
- [4] A.S. Bolina, W.A. Brown, Studies of physisorbed ammonia overlayers adsorbed on graphite, *Surf. Sci.* 598 (2005) 45-56.
- [5] S.E. Bisschop, H.J. Fraser, K.I. Öberg, E.F. van Dishoeck, S. Schlemmer, Desorption rates and sticking coefficients for CO and N₂ interstellar ices, *Astron. Astrophys.* 449 (2006) 1297-1309.
- [6] K. Acharyya, G.W. Fuchs, H.J. Fraser, E.F. van Dishoeck, H. Linnartz, Desorption of CO and O₂ interstellar ice analogs, *Astron. Astrophys.* 466 (2007) 1005-1012.
- [7] J.A.W. Elliott, C.A. Ward, Temperature programmed desorption: A statistical rate theory approach, *J. Chem. Phys.* 106 (1997) 5677-5684.
- [8] A.K. Galwey, M.E. Brown, Application of the Arrhenius equation to solid state kinetics: can this be justified?, *Thermochim. Acta* 386 (2002) 91-98.
- [9] R. Luna, C. Millán, M. Domingo, C. Santonja, M.Á. Satorre, Experimental study of the frequency factor in the Polanyi-Wigner equation: The case of C₂H₆, *Vac.* 122 (2015) 154-160.
- [10] R. Luna, M.Á. Satorre, M. Domingo, C. Millán, R. Luna-Ferrándiz, G. Gisbert, C. Santonja, Thermal desorption of methanol in hot cores. Study with a quartz crystal microbalance, *Mon. Not. R. Astron. Soc.* 473 (2018) 1967-1976.
- [11] M.Á. Satorre, M. Domingo, C. Millán, R. Luna, R. Vilaplana, C. Santonja, Density of CH₄, N₂ and CO₂ ices at different temperatures of deposition. *Planet. Space Sci.* 56 (2008) 1748-1752.
- [12] G. Sauerbrey, The use of quartz crystal oscillators for weighing thin layers and for micro-weighing, *Z. Physik* 155 (1959) 206-222.
- [13] R. Luna, C. Millán, C. Santonja, M.Á. Satorre, Triple test under high vacuum conditions to control the reliability of thin ice film accretion and desorption for astrophysical applications, *Vac.* 83 (2009) 942-948.